

DEVELOPMENT OF A NONLINEAR INDICIAL MODEL FOR MANEUVERING FIGHTER AIRCRAFT

Patrick H. Reisenhel¹
Nielsen Engineering & Research, Inc.
Mountain View, CA

ABSTRACT

A nonlinear indicial prediction model was developed to predict the unsteady aerodynamic response associated with maneuvering flight vehicles at high angles of attack. The model is based on nonlinear indicial response theory and key simplifications thereof using functional interpolation of parameterized responses. This paper presents the initial development of the method and its application to a model problem involving the "Cobra" maneuver by a full-scale fighter aircraft.

NOMENCLATURE

Symbols and abbreviations

B	Box function
c	Wing chord
d_{pnk}	Functional interpolation coefficients
C_L	Lift coefficient
C_z	Vertical force coefficient
GK	Goman-Khrabrov
H	Heaviside step function
q	Pitch rate
QS	Quasi-static
t	Time
t^*	Time at which the indicial step is applied
U_∞	Freestream velocity
x	Internal state variable
α	Angle of attack
δ_{ij}	Kroenecker delta
ϕ	Roll angle
τ	Auxiliary time variable
τ_c	Time at which critical state is crossed
ξ	Parameter denoting dependence on prior motion history

Subscripts

CS	Critical state
dyn	Dynamic
max	Maximum
qs	Quasi-static
∞	Time-asymptotic value (except for U_∞)

Superscripts

\bullet	Derivative with respect to time
$\bullet\bullet$	Second derivative with respect to time
\sim	Indicial function
$-$	Mean
$*$	Evaluation at the time of the indicial step
\frown	Interpolated value

1. INTRODUCTION

In recent years, it has been possible to integrate the flight-dynamics equations fairly efficiently using linearized aerodynamics which are occasionally supplemented with ad hoc methods (i.e., semi-empirical simulations or wind tunnel data) to include nonlinear unsteady aerodynamic effects. With the expanded flight envelopes being considered for future maneuvering aircraft, it has become increasingly important to be able to model and predict nonlinear, unsteady aerodynamics. This includes the prediction of the aerodynamic response in the presence of flow separation, shock movement, and vortex bursting, among other phenomena, at high angles of attack and/or high angular rates. Existing flow prediction methods are either too expensive or lack the proper fidelity to represent the physics of the aerodynamic flow. A consequence of the poor modeling fidelity is a greater design uncertainty, lack of performance, and, possibly, expensive redesigns

¹ Chief Scientist, Member AIAA

and retrofits of existing fleet vehicles, such as the F-18.

Future fighter aircraft will be required to perform controlled maneuvers well beyond traditional aircraft limits, for example, pitch up and flight at high angles of attack, rapid point-to-shoot, and other close-in combat maneuvers. To perform these ultrafast multi-axis motions, future tactical aircraft and missiles will pioneer the use of innovative technologies such as thrust vectoring control. To produce the best aircraft for these extreme flight conditions, it is necessary to combine successfully several disciplines in the design phase of the aircraft: flight mechanics, unsteady aerodynamics, flexible structural modeling, and control system simulation/design. The anticipated advanced maneuvers demand the use of aerodynamic methods capable of predicting characteristics of the nonlinear post-stall regime for multi-axis motions at extremely high rates.

2. OBJECTIVE AND APPROACH

In order to predict the dynamics of maneuvering aircraft or missiles at high rotational rates and high angles of attack, it is essential to accurately and efficiently model the nonlinearities associated with post-stall aerodynamics, including bifurcations and hysteresis. Nonlinear indicial theory offers a viable alternative which can fulfill the need for the efficient and accurate modeling of nonlinear "plant" characteristics. The knowledge of these characteristics is a prerequisite for structural response feedback techniques and control system configuration system design. The goal of this effort is to provide an unsteady aerodynamic model based on nonlinear indicial response theory. An important note concerning the application of nonlinear indicial theory is that the indicial functions (responses) can be obtained from numerical computations, experimental tests, or by analytic means, whichever is appropriate or available.

The present paper is the first of two papers based on the present study. The validation of the nonlinear indicial approach for predicting the unsteady aerodynamic loads at high α was performed on two distinct models for the unsteady aerodynamic responses. The first model (and the topic of this first paper) is a two-parameter delay differential equation model approximating the pitch plane high angle-of-attack maneuvering of a fighter aircraft (full scale).

The second model (and the topic of the second paper, Ref. 14) is an artificial neural network which was trained to reproduce the high angle-of-attack aerodynamic characteristics of a pitching rectangular wing (wind tunnel test, Ref. 23).

3. BACKGROUND

3.1. Linear Indicial Theory

The indicial approach is based on the concept that a characteristic flow variable $f(\bar{x}, t)$, which describes the state of the flow, can be linearized with respect to its boundary condition (or forcing function), $\epsilon(t)$, if the variation of $f(\bar{x}, t)$ is a smooth function of $\epsilon(t)$. This allows the representation of $f(\bar{x}, t)$ in a Taylor series about some value of $\epsilon = \epsilon_0$; thus

$$f(\bar{x}, t) = f(\bar{x}, 0) + \Delta \epsilon \left. \frac{\partial f}{\partial \epsilon} \right|_{\epsilon=\epsilon_0} + \dots$$

If $f(\bar{x}, 0)$ is zero (a zero initial condition), then an approximate solution is

$$f(\bar{x}, t) = \Delta \epsilon \left. \frac{\partial f}{\partial \epsilon} \right|_{\epsilon=\epsilon_0} \quad (1)$$

Equation (1) is an approximation which becomes more accurate as $\Delta \epsilon \rightarrow 0$. Also, Eq. (1) is exact if $f(\bar{x}, t)$ is a linear function of $\epsilon(t)$. If the response $\partial f / \partial \epsilon$ depends only on the elapsed time from the perturbation $\Delta \epsilon$ (a linear time invariant response) then it may be shown (Ref. 1) that the formal solution for $f(\bar{x}, t)$ is

$$f(\bar{x}, t) = \tilde{f}(\bar{x}, t) \epsilon(0) + \int_0^t \frac{d\epsilon}{d\tau} \tilde{f}(\bar{x}, t-\tau) d\tau \quad (2)$$

$$\text{where } \tilde{f}(\bar{x}, t) = \left. \frac{\partial f}{\partial \epsilon} \right|_{\epsilon=\epsilon_0}.$$

Hence, if the forcing function (i.e., the boundary condition ϵ) is known and if \tilde{f} is known from some computation or experimental determination, then Eq. (2) gives the value of $f(\bar{x}, t)$ for any schedule of boundary conditions $\epsilon(t)$ without the need to compute f from first principles. This has the effect

of reducing computational costs considerably. Equation (2) is a semi-analytic relation between $f(\bar{\mathbf{x}}, t)$ and its boundary condition or forcing function $\mathbf{E}(t)$. The symbol $\bar{\mathbf{x}}$ represents a set of independent variables x_i such as spatial coordinates. For simplicity, if these variables do not depend on time, they (x_i) are omitted in subsequent discussions.

The power of linear indicial theory is that if a system can be approximated as linear time-invariant, then the knowledge of only the indicial functions of the system suffices to determine its response to any arbitrary schedule of its boundary conditions. This leads to a tremendous reduction in computational requirements. In particular, in the case where the indicial functions can themselves be further approximated (e.g., via exponential fits), then it may be shown (Ref. 2) that the entire unsteady aerodynamic prediction amounts to solving a low-dimensional system of inhomogeneous coupled first order ordinary differential equations.

As a general rule, linear indicial theory is valid away from bifurcations such as changes in flow topology, and provided that the perturbation displacements are small. Linear indicial theory has been validated in numerous examples ranging from unsteady transonic flow around airfoils (Ref. 3) and missile bodies (Ref. 4) to separated viscous flow at low Reynolds numbers (Ref. 5). More recently, the nonlinear flow associated with finite amplitude perturbations ($\Delta\alpha \approx 5^\circ$) relative to a reference pitching motion was shown to be predicted accurately using Navier-Stokes indicial functions inferred in the Laplace domain (Ref. 6).

3.2. The Volterra Series Approach

It would be ideal to use indicial theory for the treatment of high alpha aerodynamics of a maneuvering aircraft. However, there are several difficulties with this approach. The first difficulty is that it does not apply to systems for which the underlying assumption of time-linear invariance breaks down. When nonlinear effects become important, such as in the case of the appearance of a shock wave or with any topological change of the flowfield (e.g., separation onset, appearance/disappearance of separation bubbles, burst vortex, etc.), the indicial approach becomes inaccurate. Such evidence can be found, for example, in the studies of Refs. 3 and 6.

In general, the linear indicial method cannot handle multiple solutions, bifurcations, jumps, and other nonlinear phenomena which typically occur in high angle-of-attack vortical flows. Another difficulty is that the flowfields of interest are characterized by a significant amount of hysteresis, i.e., the effects of the past history of the flow are considerable. This violates the assumptions which underlie the use of linear indicial theory because the linear indicial functions do not contain any memory effects, and depend only on the instantaneous state of the system.

To overcome these deficiencies, it has been proposed (Refs. 7, 8) to use a Volterra series approach in order to capture the nonlinear aerodynamic response. The theory behind the Volterra series methodology asserts that the response of a nonlinear time invariant system can be represented exactly as an infinite sum of multidimensional convolution integrals, of which the first term (linear kernel) is analogous to the linear indicial theoretical formulation:

$$\begin{aligned} f(t) = & \int_0^t \chi_1(t-\tau_1) \mathbf{e}(\tau_1) d\tau_1 \\ & + \int_0^t \int_0^{\tau_1} \chi_2(t-\tau_1, t-\tau_2) \mathbf{e}(\tau_1) \mathbf{e}(\tau_2) d\tau_1 d\tau_2 \\ & + \int_0^t \int_0^{\tau_1} \int_0^{\tau_2} \chi_3(t-\tau_1, t-\tau_2, t-\tau_3) \times \\ & \quad \mathbf{e}(\tau_1) \mathbf{e}(\tau_2) \mathbf{e}(\tau_3) d\tau_1 d\tau_2 d\tau_3 + \dots \\ & + \int_0^t \dots \int_0^{\tau_1} \chi_n(t-\tau_1, t-\tau_2, \dots, t-\tau_n) \times \\ & \quad \mathbf{e}(\tau_1) \dots \mathbf{e}(\tau_n) d\tau_1 \dots d\tau_n + \dots \end{aligned}$$

The Volterra theory approach derives from the considerable body of work that has been done in connection with the modeling of nonlinear systems "with memory" (Ref. 7). The recent interest in modeling unsteady nonlinear aerodynamics by this approach has mostly focused attention on the identification of the so-called Volterra kernels (χ_n) in both the Laplace (Refs. 7, 9) and time domain (Ref. 8). However, these efforts have been limited so far to the identification of first and second order kernels only. This is because of the considerable work/expense involved in their determination (see for instance Ref. 8). As previously recognized by Tromp and Jenkins (Ref. 7) the Volterra series approach to modeling only has practical value if the number of

terms necessary to represent the system is small. This amounts to restricting the method to the modeling of *weakly nonlinear* systems.

Although the Volterra kernel identification method shows promise at this time for the aerodynamic modeling of weakly nonlinear configurations, these methods are in their infancy and generally lack practicality for routine aerodynamic simulations.

3.3. Nonlinear Indicjal Theory

The basic idea behind the use of nonlinear indicjal functions, as defined by Tobak et al. (Ref. 10) and Tobak and Chapman (Ref. 11) is that the linear formalism, Eq. (2), can be retained in the form of a generalized superposition integral, provided that the nonlinear indicjal response \tilde{f} is now taken to be a functional $\tilde{f}(\boldsymbol{\epsilon}(\xi); t, \tau)$, where $\boldsymbol{\epsilon}(\xi)$ denotes the dependence on the entire motion history:

$$f(t) = f(t; \boldsymbol{\epsilon}(0)) + \int_0^t \frac{d\boldsymbol{\epsilon}}{d\tau} \tilde{f}(\boldsymbol{\epsilon}(\xi); t, \tau) d\tau \quad (3)$$

Equation (3) is, therefore, a generalization of the linear convolution model (Duhamel convolution integral), Eq. (2). It was formally shown that this formulation is equivalent to a nonlinear functional expansion of which the classical Volterra series is a subset. In the nonlinear indicjal formulation, the nonlinear indicjal function $\tilde{f}(\boldsymbol{\epsilon}(\xi); t, \tau)$ is defined as the following Fréchet derivative:

$$\begin{aligned} \tilde{f}(\boldsymbol{\epsilon}(\xi); t, \tau) &= \lim_{\Delta \boldsymbol{\epsilon} \rightarrow 0} \frac{\Delta f(t)}{\Delta \boldsymbol{\epsilon}} \\ &= \lim_{\Delta \boldsymbol{\epsilon} \rightarrow 0} \left[\frac{f(\boldsymbol{\epsilon}(\xi) + H(\xi - \tau) \Delta \boldsymbol{\epsilon}) - f(\boldsymbol{\epsilon}(\xi))}{\Delta \boldsymbol{\epsilon}} \right] \end{aligned}$$

where the step in boundary condition, $\Delta \boldsymbol{\epsilon}$, is applied at time $t = \tau$, and H designates the Heaviside step function.

Note from Eqs. (2) and (3) that the linear and nonlinear indicjal function approaches formally differ fundamentally in two ways. First, the fact that $\tilde{f}(\boldsymbol{\epsilon}(\xi); t, \tau)$ has a separate dependence on t and τ rather than on the elapsed time $(t - \tau)$ alone signifies that \tilde{f} in the nonlinear formulation can now depend

on the past history of the boundary conditions, i.e., "memory" effects are included in the kernel. Second, the functional dependency on $\boldsymbol{\epsilon}(\xi)$ itself distinguishes the nonlinear indicjal response from its linear counterpart. In practice, the quantity f of interest might typically be an integrated load (e.g., C_L) or generalized aerodynamic force (for flexible bodies), while the boundary condition $\boldsymbol{\epsilon}$ might be an aeroelastic modal amplitude, or the angle of attack, α . In the latter case, the generalized superposition integral, Eq. (3), may express the full dependence of C_L on prior motion, given any arbitrary schedule of $\alpha(t)$. This formalism is formally valid as long as f remains Fréchet-differentiable, a condition which is violated at bifurcation points.

In order to address this point, Tobak and Chapman (Ref. 11) modified the theory so as to include bifurcation points. These are identified as discrete points during the aircraft motion at which Fréchet differentiability is lost. This can be due to the loss of stability of a particular solution (or equilibrium state prior to the bifurcation) changing to a new equilibrium state which is stable. This discrete change to a new equilibrium at the critical (bifurcation) time τ_c is accommodated in the theory by splitting the generalized superposition integral as follows

$$\begin{aligned} f(t) &= f(t; \boldsymbol{\epsilon}(0)) + \int_0^{\tau_c} \frac{d\boldsymbol{\epsilon}}{d\tau} \tilde{f}(\boldsymbol{\epsilon}(\xi); t, \tau) d\tau \\ &\quad + \Delta f(t; \boldsymbol{\epsilon}(\tau_c)) + \int_{\tau_c}^t \frac{d\boldsymbol{\epsilon}}{d\tau} \tilde{f}(\boldsymbol{\epsilon}(\xi); t, \tau) d\tau \end{aligned}$$

where

$$\begin{aligned} \Delta f(t; \boldsymbol{\epsilon}(\tau_c)) &= f(\boldsymbol{\epsilon}(\xi); t, \tau_c + \delta\tau) \\ &\quad - f(\boldsymbol{\epsilon}(\xi); t, \tau_c - \delta\tau) \end{aligned}$$

is taken in the limit: $\delta\tau \rightarrow 0$. The term $\Delta f(t; \boldsymbol{\epsilon}(\tau_c))$ represents the possibility of a discontinuous jump. Recent work (Ref. 12) at Wright Laboratory has shown, for example, that when a critical state of the flow is crossed, this gives rise to unusually long transients. These long transients are believed to be associated with the jump response, $\Delta f(t; \boldsymbol{\epsilon}(\tau_c))$.

4. NONLINEAR INDICJAL MODEL

The basis of the nonlinear indicjal response model is the generalized superposition integral which, in the absence of bifurcations, can be expressed according to

Eq. (3), i.e.,

$$\mathbf{f}(t) = \mathbf{f}(t; \mathbf{e}(0)) + \int_0^t \frac{d\mathbf{e}}{d\tau} \tilde{\mathbf{f}}(\mathbf{e}(\xi); t, \tau) d\tau$$

where the functional $\tilde{\mathbf{f}}(\mathbf{e}(\xi); t, \tau)$ is the nonlinear indicial response and $\mathbf{e}(\xi)$ denotes the dependence on the entire prior motion history. If the system is linear time-invariant, i.e., if

$$\tilde{\mathbf{f}}(\mathbf{e}(\xi); t, \tau) \equiv \tilde{\mathbf{f}}(t-\tau)$$

then Eq. (3) is the familiar Duhamel convolution integral (linear indicial theory), Eq. (2).

If it is assumed that the general nonlinear indicial response $\tilde{\mathbf{f}}(\mathbf{e}(\xi); t, \tau)$ can be simplified based on a suitable parameterization (which may include, for instance, only the recent time history), then the nonlinear indicial response may be expressed as

$$\tilde{\mathbf{f}}(\mathbf{e}(\xi); t, \tau) \approx \tilde{\mathbf{f}}_{\mathbf{e}, \tau}(t-\tau)$$

In other words, just as in the linear formulation, the indicial function depends only on the elapsed time $(t-\tau)$, provided, however, that the functional form $\tilde{\mathbf{f}}_{\mathbf{e}, \tau}$ be determined according to parameters which adequately describe its dependence on the recent motion history at time τ (for example: $\alpha(\tau)$, in a constant $\dot{\alpha}$ maneuver).

Thus, for example, the continuous global response for the lift coefficient, C_L , is given by

$$C_L(t) = C_L(0) + \int_0^t \left[\frac{\delta C_L(t-\tau)}{\delta \alpha} \right]_{\tau} \frac{d\alpha}{d\tau} d\tau \quad (4)$$

where $(\delta C_L / \delta \alpha)_{\tau}$ designates the indicial response resulting from an elementary perturbation applied at time τ during the maneuver. Alternatively, $(\delta C_L / \delta \alpha)_{\tau}$ is the local approximation of the indicial function around $\alpha = \alpha_M(\tau)$, where $\alpha_M(t)$ is the reference motion which was used to determine the indicial responses.

It would be ideal to compute the generalized convolution integral, Eq. (4), analytically. This is

possible if, for example, $(\delta C_L / \delta \alpha)_{\tau}$ can be fitted in some way. However, the lack of smoothness of the indicial function space generally precludes such an approach. Instead, a numerical integration of (4) is sought.

In a discrete system, the indicial responses $(\delta C_L / \delta \alpha)_{\tau}$ are not known or available at every time instant τ of the maneuver. We start by considering the case where it is assumed that a finite number of indicial responses have been determined along a given trajectory $\alpha_M(t)$. In this scenario, the time axis can be formally partitioned so that each partition $[t_{k-1}, t_k]$ is assigned one representative indicial function, denoted for example $(\delta C_L / \delta \alpha)_k$ for the lift coefficient. This results in a global indicial function $(\delta C_L / \delta \alpha)_{\tau}$ which can be formally written as

$$\left[\frac{\delta C_L(t-\tau)}{\delta \alpha} \right]_{\tau} = \sum_{k=1}^{+\infty} \left[\frac{\delta C_L(t-\tau)}{\delta \alpha} \right]_k B_k(\tau) \quad (5)$$

where B_k is a "Box function," defined as

$$B_k(\tau) \equiv H(\tau - t_{k-1}) - H(\tau - t_k)$$

Equations (4) and (5) are the analog of the linear indicial formulation for a system which is no longer linear time invariant in a global sense. This is expressed by the fact that the kernel of the Duhamel convolution integral is not a function of $(t-\tau)$ alone but of both variables t and τ independently. Note also that the functional dependency on $\mathbf{e}(\xi)$ (in Eq. (3)) is implicit, through the specification of the nonlinear switching points, $\{t_k\}$, of the partition.

Equation (4) is the lowest order implementation of nonlinear indicial theory. It corresponds to a "piecewise-linear" indicial theory. To construct higher order (and presumably more accurate) models, it is useful to look at Eq. (4) in terms of functional interpolation. The piecewise-linear mode relies upon a zeroth-order interpolation of the indicial responses themselves. A somewhat more sophisticated model, for example a first order model, would involve some form of weighted averaging based on the "distance" to the closest available indicial responses, k and $k-1$:

$$\left[\frac{\delta C_L(t-\tau)}{\delta \alpha} \right]_{\tau} = \sum_{k=1}^{+\infty} \left(\frac{t_k - \tau}{t_k - t_{k-1}} \left[\frac{\delta C_L(t-\tau)}{\delta \alpha} \right]_{k-1} + \frac{\tau - t_{k-1}}{t_k - t_{k-1}} \left[\frac{\delta C_L(t-\tau)}{\delta \alpha} \right]_k \right) B_k(\tau) \quad (6)$$

A straightforward generalization of Eqs. (5) and (6) for a number of weighted linear interpolation schemes is given by

$$\left[\frac{\delta C_L(t-\tau)}{\delta \alpha} \right]_{\tau} = \sum_{k=1}^{+\infty} \left[\sum_{p=1}^{+\infty} d_{pk}(\tau) \left[\frac{\delta C_L(t-\tau)}{\delta \alpha} \right]_p \right] B_k(\tau) \quad (7)$$

where $d_{pk}(\tau)$ are interpolation coefficients. For zeroth-order interpolation only one nonzero coefficient is required ($d_{pk}(\tau) = \delta_{pk}$); for linear interpolation, two nonzero $d_{pk}(\tau)$'s are to be calculated, and so on.

Nonlinear functional interpolation schemes were also considered as part of this study. Examples include quadratic and spline interpolation schemes. The specific methods are discussed in Ref. 13. Generally speaking, these schemes can be expressed as a straightforward extension of Eq. (7), i.e.:

$$\left[\frac{\delta C_L(t-\tau)}{\delta \alpha} \right]_{\tau} = \sum_{k=1}^{+\infty} \left[\sum_{p=1}^{+\infty} \left[\sum_{n=1}^{n=N} d_{pnk}(\tau) \left[\frac{\delta C_L(t-\tau)}{\delta \alpha} \right]_p^n \right] \right] B_k(\tau) \quad (8)$$

When dealing with novel motions for which no indicial function is available, the concept of univariate interpolation in time must be replaced by multivariate interpolation schemes of the minimum number of parameters needed to characterize the indicial function space. The formalism of Eq. (8) can be retained, provided that a few definitional changes be made. For example, if the five instantaneous parameters $\alpha, \dot{\alpha}, \phi, \dot{\phi}$ and $\ddot{\phi}$ are required, then the concept of box function must be extended in five-dimensional space, i.e.,

$$B_k(\tau) \equiv \bar{B}_k(\alpha) \bar{B}_k(\dot{\alpha}) \bar{B}_k(\phi) \bar{B}_k(\dot{\phi}) \bar{B}_k(\ddot{\phi})$$

In the above notation, it is understood that, for any given parameter $\mu(t)$, the following definition is used:

$$\bar{B}_k(\mu) \equiv H(\mu - \mu_{k-1}) - H(\mu - \mu_k)$$

where the functional interpolation nodes μ_k represent an ordered partition of the indicial function space in the μ -direction, such that

$$t_{k-1} \leq \tau < t_k \Rightarrow \mu(\tau) \in [\mu_{k-1}, \mu_k)$$

Similarly, the interpolation weights, $d_{pnk}(\tau)$, will now depend on the distance between the point $(\alpha, \dot{\alpha}, \phi, \dot{\phi}, \ddot{\phi})$ at time τ and the interpolation nodes (multivariate partition) in parameter space.

5. METHOD

The development, testing, and validation of the nonlinear indicial prediction model require large amounts of unsteady aerodynamic data. Unsteady aerodynamic responses are necessary, both to generate the required indicial functions and/or critical state responses, and to compare the indicial theoretical prediction to the data for arbitrary maneuvers.

It would be ideal to use unsteady aerodynamic responses inferred from experimental tests. At this time, however, many of the practical problems involved in extracting such information have not been resolved. An alternative is the use of Computational Fluid Dynamics (CFD), but this approach is expensive and impractical.

The approach taken in the present research has been to consider, instead, the use of efficient and, hopefully, reasonably accurate nonlinear models for the unsteady flow behavior. Specifically, two models were considered. The first model (referred to as the Goman-Khrabrov model) is an analytical model which approximates the flight test aerodynamic responses of a fighter aircraft undergoing "Cobra"-type maneuvers. The application of nonlinear indicial theory to this first example (i.e., the Goman-Khrabrov model) is the topic of the present paper. The second model is an artificial neural network which was trained on wind tunnel data of a pitching rectangular wing undergoing dynamic stall. This second example is much more nonlinear and includes in particular a critical state or

aerodynamic bifurcation which requires special handling. The application of nonlinear indicial theory to the neural network example is the topic of a future paper (Ref. 14).

To avoid any possible confusion, from here on the term "model" will be reserved for the nonlinear indicial prediction scheme outlined in the previous section, i.e., (combining Eqs. (4) and (8), and including the possibility of a jump response):

$$\begin{aligned}
 C_L(t) - C_L(0) = & \quad (9) \\
 & \int_0^{\tau_c - \epsilon} \sum_{k=1}^{+\infty} \left[\sum_{p=1}^{+\infty} \left[\sum_{n=1}^{n=N} d_{pnk}(\tau) \times \right. \right. \\
 & \quad \left. \left. \left[\frac{\delta C_L(t-\tau)}{\delta \alpha} \right]_p^n \right] \right] B_k(\tau) \frac{d\alpha}{d\tau} d\tau \\
 & + \Delta C_L^{CS}(t; \alpha(\tau_c)) \\
 & + \int_{\tau_c + \epsilon}^t \sum_{k=1}^{+\infty} \left[\sum_{p=1}^{+\infty} \left[\sum_{n=1}^{n=N} d_{pnk}(\tau) \times \right. \right. \\
 & \quad \left. \left. \left[\frac{\delta C_L(t-\tau)}{\delta \alpha} \right]_p^n \right] \right] B_k(\tau) \frac{d\alpha}{d\tau} d\tau
 \end{aligned}$$

in the case of the lift coefficient. By contrast, the Goman-Khrabrov and neural network "models" (in the old terminology) will be referred to as "systems," since they approximate the behavior of real fluid systems (a pitching aircraft or a pitching wing). Accordingly, the output of these systems will be referred to as the "data," as opposed to the "prediction," which is the output of the indicial model.

The Goman-Khrabrov and neural network systems both exhibit complex nonlinear behavior. In each case, they are used (1) to generate the indicial and (if present) critical-state-response data, and (2) to compare against the indicial theoretical prediction for novel maneuvers. The application of the indicial theoretical prediction method to the Goman-Khrabrov system is described below.

6. APPLICATION OF THE METHOD TO THE GOMAN-KHRABROV SYSTEM

6.1. Description of the Goman-Khrabrov System

The Goman-Khrabrov system (abbreviated "GK") is a mathematical model which was shown (Ref. 15) to accurately describe unsteady aerodynamic effects observed in several experimental investigations,

including unsteady flow about an airfoil with trailing-edge separation (Ref. 16), a delta wing with vortex breakdown (Ref. 17), and a maneuvering fighter aircraft (Ref. 15). The model extends the usual flight dynamics equations by introducing a first order delay differential equation for an additional internal state variable x which accounts for unsteady effects associated with separated and vortex flow. The variable x may, for instance, represent the location of flow separation or that of vortex breakdown. The form of the differential equation governing x is:

$$\tau_1 \frac{dx}{dt} + x = x_0(\alpha - \tau_2 \frac{d\alpha}{dt}) \quad (10)$$

where α is the angle of attack, τ_1 and τ_2 are time constants, and x_0 describes the steady dependency of x on α . The rationale for the model as well as the details of the model can be found in Ref. 15. For the present purpose, it suffices to say that τ_2 defines a quasi-static time delay associated with "changes in circulation, boundary layer convection lags, and/or boundary layer improvement effects," while τ_1 is a relaxation time constant associated with global transient aerodynamic effects, or "dynamic properties of the separated flow adjustment." The parameters τ_1 and τ_2 are different for different flowfields and must be determined using parameter identification techniques.

For a complete representation one must, of course, link the force coefficient(s) to the motion parameters, and the introduction of an internal state-space variable is claimed to facilitate this task considerably. The system considered here is that of a full-scale fighter aircraft undergoing the well-known "Cobra" maneuver (Ref. 18). Goman and Khrabrov use the following model for the vertical force coefficient C_z :

$$\begin{aligned}
 C_z = & C_z^{nl}(\alpha, x) + C_{z_q}^{att} \frac{qc}{U_\infty} \\
 & + C_{z_\alpha}^{att} \frac{d\alpha}{dt} \frac{c}{U_\infty} + C_{z_{\delta_e}} \delta_e
 \end{aligned}$$

where the *att* superscript denotes the component due to attached flow, *nl* is the nonlinear function, q is pitch rate, c is the wing mean aerodynamic chord, and δ_e is the elevator deflection. The nonlinear component C_z^{nl} is modeled simply as

$$C_z^{nl}(\alpha, \mathbf{x}) = C_{z_1}(\alpha) g(\mathbf{x}) + C_{z_2}(\alpha) (1 - g(\mathbf{x})) \quad (11)$$

where C_{z_1} and C_{z_2} designate envelope curves for C_z for $d\alpha/dt > 0$ and $d\alpha/dt < 0$, respectively, and $g(\mathbf{x})$ is a normalized weight function.

The authors obtained good agreement between this model and flight test data for a maneuvering aircraft, assumed to be an Su-27. The two aircraft maneuvers shown in Ref. 15 were analytically approximated as shown in Fig. 1. The first maneuver is a pitch up from $\alpha \approx 7^\circ$ to $\alpha \approx 90^\circ$, then back down to $\alpha \approx 7^\circ$, over a total time period of approximately 6 seconds. The second maneuver is similar but only pitches up to about 60° angle-of-attack over a period of 10 seconds or so. A simple parameter identification analysis was performed by systematically varying the model constants until our predictions (using Eq. 11) approximately matched those of Ref. 15 for both aircraft maneuvers. The delay differential equation, Eq. (10), was integrated using the Fehlberg fourth-fifth order Runge-Kutta method (Ref. 19). The result is shown in Fig. 2, which is the analog of Goman and Khrabrov's (1994) Fig. 13. Actual values for the model constants used are given in Ref. 13. The lower hysteresis loops in Fig. 2 correspond to $x(\alpha)$, parameterized by time. The pairs of loops in the upper portion of Fig. 2 are the hysteresis curves for C_z , corresponding to the GK model prediction (solid lines). For both the C_z and x curves, the static curves (C_z^{st} and x_0) are indicated for reference (dashed lines).

6.2. Indicial Function Determination

The basic procedure for determining the indicial responses of the Goman-Khrabrov system is illustrated in Fig. 3. In this example, the indicial response is determined for a perturbation $\delta\alpha$ introduced at time $\tau \approx 7$ (i.e., around $\alpha = 46^\circ$ during the pitch down portion of the 90° Cobra maneuver illustrated in Fig. 1). Following the definition of the indicial response, two almost identical maneuvers $\alpha_1(t)$ and $\alpha_2(t)$ are carried out. The two maneuvers coincide with the Cobra maneuver for $t < \tau$. At $t = \tau$, the motion is stopped for the first maneuver ($\alpha_1(t) = \alpha_1(\tau)$, for $t \geq \tau$). The second maneuver is similarly stopped, except that the angle of attack is incremented by $\delta\alpha$ at time τ ($\alpha_2(t) = \alpha_2(\tau) + \delta\alpha$, for

$t \geq \tau$). Let $C_{z_1}(t)$ and $C_{z_2}(t)$ denote the aerodynamic responses associated with $\alpha_1(t)$ and $\alpha_2(t)$, respectively. The indicial response is calculated as²

$$\begin{aligned} \tilde{C}_z(t-\tau) &\equiv \frac{\delta C_z(t-\tau)}{\delta\alpha} \\ &\approx \frac{C_{z_2}(t) - C_{z_1}(t)}{\delta\alpha} H(t-\tau) \end{aligned}$$

This technique is referred to as the direct technique. It is a straightforward application of the definition of the indicial function as a Fréchet derivative, and requires (1) that infinite rates be produced at $t = \tau$, and (2) that $\delta\alpha$ be infinitesimal. Because of these constraints, the direct technique cannot be used experimentally, and also causes serious difficulties with CFD. Under these circumstances, an alternative method must be used. For example, we have shown (Ref. 6) that it is possible to correctly infer the indicial response by using inverse Laplace transform techniques. These were successfully applied to cases where $\alpha_2(t) - \alpha_1(t)$ for $t \geq \tau$ is neither constant nor infinitesimal.

To make use of the direct technique in a discrete system, one must ensure (1) that the results are convergent for $\delta\alpha \rightarrow 0$, and (2) that they are also convergent for $\Delta t \rightarrow 0$. Both of these tests are easily met in the Goman-Khrabrov system. For example, the convergence of the indicial response with the integration time step (in seconds) is illustrated in Fig. 4. The parameters $\Delta t = 0.01$ and $\delta\alpha = 0.01^\circ$ were selected for the remainder of the GK system study.

Examples of indicial responses calculated at various points throughout the large amplitude ($\alpha_{\max} = 90^\circ$ "Cobra") maneuver are shown in Figs. 5a and 5b. Note that, for clarity, the indicial functions plotted in Fig. 5 are time-shifted according to the time instant at which the perturbation $\delta\alpha$ is applied (i.e., $\tau=0$ corresponds to $t=\tau$). Note also that the indicial responses $\delta C_z/\delta\alpha$ are in units of inverse degrees. It should be clear from the result of Fig. 5 that the indicial response is not only a function of the instantaneous angle of attack, but indeed of the prior

² Note that, in the case of the Goman-Khrabrov system, the indicial responses can also be calculated analytically (see Ref. 13)

motion history. For example, the last six indicial responses (labeled " $\alpha = 7^\circ$ ") in Fig. 5b all correspond to a portion of the maneuver where the angle of attack remains unchanged. Yet, the indicial responses exhibit significant variations.

6.3. Test of the Indicial Method

There are two levels of testing of the indicial theoretical prediction. The first level (discussed here) involves reproducing the very maneuver from which the indicial responses were determined, prior to the indicial step. In this manner, one has the opportunity to test two requirements: (1) the validity of the basic formulation (Eq. 4), and (2) the ability to approximate Eq. (4) via functional interpolation. In other words, the first level of testing examines the feasibility of smoothly blending a finite number of discrete indicial functions (for example, via Eq. (6)) to predict the unsteady aerodynamic response in the case where these indicial responses are known exactly. By "known exactly" we mean that there should not be any error or uncertainty in the indicial function due to effects of prior motion history. Such issues are addressed by the second level of testing (Section 6.7), in which one attempts to use blind indicial responses recorded for well-defined prior motion histories in order to predict the unsteady aerodynamic response associated with completely novel maneuvers.

6.4. Critical State

Prior to engaging in the testing of the accuracy of the model, it is essential to know whether or not critical states are encountered, since the convolution integral will then have to be split (Eq. (9)). Unlike the neural network example examined in Refs. 13 and 14, the Goman-Khrabrov system can be shown not to have any critical states. The proof is straightforward. It involves computing the indicial functions analytically and searching for singularities. Details of some of the key derivations are provided in Ref. 13 and are not included in the present paper. Note that the absence of aerodynamic bifurcations in the Goman-Khrabrov system pertains to the mathematical representation of the aerodynamics and does not in any way suggest their absence in the real flowfield. The main point for the present purpose is that the simplified version of nonlinear indicial theory can be tested in this example in isolation from any issues related to the inclusion of critical state (jump) responses.

Using the 24 indicial responses shown in Fig. 5, the aerodynamic force build-up time history, $\Delta C_z \equiv C_z(t) - C_z(0)$ is predicted using the linear functional interpolation version of the model, i.e.:

$$\Delta C_z(t) = \int_0^t \sum_{k=1}^{K-1} \left(\frac{t_k - \tau}{t_k - t_{k-1}} \left[\frac{\delta C_z(t-\tau)}{\delta \alpha} \right]_{k-1} + \frac{\tau - t_{k-1}}{t_k - t_{k-1}} \left[\frac{\delta C_z(t-\tau)}{\delta \alpha} \right]_{k-1} \right) B_k(\tau) \frac{d\alpha(\tau)}{d\tau} d\tau \quad (12)$$

where the partition $\{t_k\}$ is defined by the midpoint between successive indicial functions. Note that the summation on k is necessarily finite, i.e., it is carried out from $k=1$ to $k=K-1$, if $t_{K-1} \leq t < t_K$. Details concerning the implementation of Eq. (12) can be found in Ref. 13. The resulting prediction using 24 indicial functions is shown in Fig. 6. It was shown (Ref. 13) that the prediction can be made arbitrarily accurate simply by choosing a sufficiently large number of indicial functions. To illustrate the importance of phase lags, if one goes through the exercise of attempting to predict the aerodynamic force build-up history, $\Delta C_z(t)$, based only on the aerodynamic derivatives $[\delta C_z / \delta \alpha]_{\tau=\infty}$ (i.e., by treating the indicial responses as step functions simulating an instantaneous response (no phase lags)), then the curve labeled "quasi-steady" is obtained (see Fig. 6). Thus, unsteady effects are responsible for the asymmetric nature of the response with respect to α_{\max} and for the dynamic overshoot ($[\Delta C_z]_{\max} \approx 1.9$) with respect to the quasi-static prediction ($[\Delta C_z]_{\max,qs} \approx 1.1$).

6.5. Parameterization of the Indicial Function Space

The true test of the indicial method lies in the ability to predict unsteady aerodynamic responses for completely new maneuvers. It may be possible to record once and for all a finite number of indicial responses, but how does one relate the indicial functions required during a novel maneuver to the pre-stored indicial responses? Indeed, the indicial approach only has value if useful simplifications can be made. A fairly intuitive idea is to assume that the indicial functions are only a function of the recent time history. Such an assumption is supported by experimental observation (see, for example, Ref. 20). It can also be proven by Taylor series arguments that,

for motions $\alpha(t)$ which are sufficiently smooth, the indicial function at time τ can be appropriately characterized using the instantaneous values of $\alpha(\tau)$, $\dot{\alpha}(\tau)$, $\ddot{\alpha}(\tau)$, $\dddot{\alpha}(\tau)$, etc. How many derivatives are required is not known, nor whether this type of projection is the most efficient one.³ A central issue is to determine what constitutes an efficient parameterization of the indicial function space. The Goman-Khrabrov system, although it is only one example, presumably represents a maneuvering aircraft and, because it is analytical, offers the opportunity to answer some of these questions and to guide the development of the method.

6.6. Motion Parameters Governing $\delta C_z/\delta \alpha$

What is important here is to note the dependencies involved in calculating $\delta C_z/\delta \alpha$. In particular, we have shown (Ref. 13) that α and $d\alpha/dt$ immediately prior to the application of the indicial step determine uniquely the indicial response $\delta x/\delta \alpha$. The fact that there is no effect of prior motion history other than α^* and $d\alpha^*/dt|_{0^-}$ is a direct consequence of the particular form of the Goman-Khrabrov delay differential equation for x . A number of other terms in the analytical evaluation of the indicial response $\delta C_z/\delta \alpha$ may also be shown to depend only on the value of α^* . Only one term is not completely determined by $(\alpha^*, d\alpha^*/dt|_{0^-})$: this "secular" term⁴ is the initial condition for $x^*(\tau)$:

$$\lim_{\tau \rightarrow 0} \{x^*(\tau)\} = x(t^*)$$

Thus,

$$\frac{\delta C_z(t-t^*)}{\delta \alpha} = f(\alpha^*, \dot{\alpha}^*, x(t^*))$$

with:

$$x(t^*) = \frac{1}{\tau_1} \int_{-\infty}^{t^*} x_0(\alpha(\zeta) - \tau_2 \dot{\alpha}(\zeta)) e^{-(t^*-\zeta)/\tau_1} d\zeta$$

³ For example, in the field of electromagnetics (Ref. 21), it is not uncommon to approximate the nonlinear impulse response as a product $g(t)h(t-\tau)g(\tau) = h(t-\tau)|_{g(\tau),g(t)}$, rather than $h(t-\tau)|_{g(\tau), dg(\tau)/dt, d^2g(\tau)/dt^2, \dots}$

⁴ The terminology is chosen to reflect the long lasting effects associated with this term, by analogy with slow time-scale terms in asymptotic expansions.

The term $x(t^*)$ describes the internal state of the system at the time the indicial step is applied. This term formally accounts for the effects of the entire prior motion history (not just the instantaneous angle of attack and pitch rate). However, due to the decaying exponential term, the effect of prior motion history is most likely restricted to several time constants τ_1 . This secular term does not affect the indicial function at large times, but is the dominant component of x^* at $\tau=0$ and, thus, will have a dominant effect at large rates.

Given that all terms other than the secular term $x(t^*)$ are determined uniquely by the instantaneous values of α and $d\alpha/dt$, the prediction error that will be incurred by using inexact indicial functions will have two possible sources.⁵ The first possible source of error is the inability to match α and $d\alpha/dt$. In other words, at a given α , the approximating indicial function must have been inferred using a maneuver which, at a minimum, must match the pitch rate at the time the indicial step is applied. The second source of error is due to error in the secular term. There, matching α and $d\alpha/dt$ is insufficient. Since matching the entire prior motion history defeats the purpose of the method, useful approximations of $x(t^*)$ must be found.

A useful way of quantifying the importance of $x(t^*)$ on the indicial function is to look at the accuracy of $\delta C_z/\delta \alpha$ at the time where it is most sensitive to $x(t^*)$ namely, at $\tau=0$. As may be seen from Fig. 7, this effect is significant. The three types of approaching indicial maneuvers considered in Fig. 7 match either α^* (with $d^m\alpha/dt^m=0, m>0$), α^* and $d\alpha^*/dt$ (with $d^m\alpha/dt^m=0, m>1$), or α^* , $d\alpha^*/dt$, and locally $d^2\alpha^*/dt^2$ (with $d^m\alpha/dt^m=0, m>2$). These approach maneuvers prior to application of the indicial step are hereafter referred to as "constant" or "zeroth order," "linear" or "first order," and "locally quadratic" or "second order," respectively. The maneuver labeled "full prediction" uses the entire prior motion history to determine $x(t^*)$ exactly. It is clear that the higher the number of derivatives matched, the more accurate the determination of the secular term, as expected from theoretical derivations.

⁵ Note that this reasoning is independent of functional interpolation error: we assume here that indicial functions are available at every point.

Next, we examine the effect of prior motion history on the unsteady aerodynamic load prediction itself. To assess the overall effect of these errors for a particular maneuver requires the application of the Duhamel convolution integral for the prediction of the force build-up, $\Delta C_z(t) = C_z(t) - C_z(0)$, namely the application of

$$\Delta C_z(t) = \int_0^t \left[\frac{\delta C_z(t-\tau)}{\delta \alpha} \right]_{\alpha} \frac{d\alpha(\tau)}{d\tau} d\tau$$

approximated by Eq. (12). The application of Eq. (12) using constant, linear, and locally quadratic approaching maneuvers for the indicial functions yields the predictions shown in Fig. 8. Note that these calculations do not involve functional interpolation in parameter space, i.e., at each time τ required in the evaluation of the integrand, $\delta C_z / \delta \alpha$ is calculated exactly (i.e., analytically, given the assumed indicial maneuver). Therefore, the comparisons shown in Fig. 8 isolate strictly the effect of assumed prior motion history of the indicial responses.

Similar tests (not shown here) were performed on different test maneuvers. Based on the results of these tests, either linear or quadratic approach indicial maneuvers seem to provide reasonable approximations. The use of higher order motion derivatives would presumably increase the accuracy further, but may not be a practical proposition.⁶ Based on the example maneuvers considered so far, a suitable compromise, in terms of accuracy, is to use the linear approach maneuver. In the following, we consider the application of the nonlinear indicial theoretical model, based only on the knowledge of indicial functions parameterized by instantaneous angle of attack α^* and pitch rate $d\alpha^*/dt$. This two-dimensional parameterization is based partly on experimental evidence (Ref. 20), partly on analysis (Ref. 13), and partly on the empirical results reported

⁶ A possible alternative is to consider α and/or $d\alpha/dt$ at a previous time, $t^* - \Delta t^*$ (Δt^* large enough), as additional parameters. Such an approach would not reduce or alter the dimensionality of the parameterization in any way, but would alleviate the dependency on "noisy" experimental determinations such as angular acceleration and other higher order derivatives.

herein. It is important to keep in mind, however, that this projection of the entire prior motion history onto a point $(\alpha, \dot{\alpha})$ is a rather severe caricature, and the model may have to be extended accordingly for different applications.

6.7. Two-Dimensional Parameterization of the Indicial Function Space

From the above results it is observed (1) that the indicial responses (and, thus, the entire prediction) involve a secular term $x(t^*)$ which depends on the entire prior motion history, and (2) that this term can be approximated reasonably accurately without knowing anything about the past history of a particular maneuver, except for the instantaneous α^* and $d\alpha^*/dt$. These observations, although limited to the Goman-Khrabrov system, suggest that it is possible to parameterize the indicial functions of the system using only α and $d\alpha/dt$.

In the present section, we consider the next step in a practical implementation of these ideas to the formulation of a nonlinear indicial model for maneuvering aircraft. In order to be practical, the method must require the use of as few indicial responses as possible. So far, the concept of functional interpolation referred to one-dimensional interpolation along the time axis. Specifically, a linear one-dimensional interpolation scheme was used (Eq. 12).

Two additional aircraft maneuvers are considered in Fig. 9. The maneuver marked "Su-27 (#1)" is the 90° cobra maneuver considered until now. The maneuver marked "Su-27 (#2)" is the second flight test maneuver shown in Fig. 1 (60° maneuver). The third maneuver is a hypothetical maneuver made of a sequence of fifth order polynomial ramps.

Without any knowledge of prior motion history, it is possible to parameterize the indicial function space in terms of α and $d\alpha/dt$ only, provided that the assumed approach indicial maneuver is of the linear type mentioned previously. In phase space, the three maneuvers shown in Fig. 9 each have a trajectory which visits a subset of this parameter space. This is shown in Fig. 10. In addition, Fig. 10 shows an example of the location of the indicial functional interpolation nodes (solid symbols). Note that the indicial maneuvers corresponding to each of the functional interpolation nodes are not shown in the

figure. These indicial maneuvers would correspond to horizontal lines (since these are "order one" approach maneuvers) and, thus, have very little in common, if any, with the three maneuvers to be predicted.

In order to provide a more complete assessment of the overall accuracy of this method, it is necessary to compare the indicial theoretical prediction with respect to the data itself (i.e., finite difference integrations of the Goman-Khrabrov system equations). Furthermore, such comparisons must be made on the basis of several maneuvers. The accuracy of the indicial theoretical prediction using the interpolation nodes shown in Fig. 10 is illustrated in Figures 11, 12, and 13. The bivariate interpolation scheme used in each case for the indicial functions is a simple piece-wise bicubic polynomial fit. A parametric study was carried out in Ref. 13. As an example, the deterioration of the prediction accuracy with increased sparseness of the indicial function space is illustrated in Fig. 14.

The particular bicubic polynomial interpolation routine used thus far requires a rectangular grid for the $(\alpha, d\alpha/dt)$ interpolation nodes. In an experimental situation (i.e., in the hypothetical case where the nonlinear indicial responses of the system might be inferred from experimental tests), indicial functions may not be available at all points of a rectangular grid in $(\alpha, d\alpha/dt)$ space. To handle this situation, one of a number of interpolation schemes for scattered data may be used. The one used here is a modified quadratic Shepard interpolation scheme (Ref. 22). In the example shown in Fig. 15, an interpolation node was removed from an irregular 6×5 grid in α and $d\alpha/dt$. The interpolation node that was removed was chosen to correspond to low angle of attack at negative pitch rate. This is known to be a sensitive part of the prediction accuracy, where large and rapid changes in x take place at reattachment. As a result, the prediction for maneuver Su27 #1 is consistently less accurate around $t=8$. The addition of noise on the location of the available indicial functions was shown not to substantially affect the quality of the prediction, which is an indication of the robustness of the method.

∴

Two key characteristics of the prediction method are emphasized. The first characteristic is its robustness, as judged by the sensitivity to the location of

interpolation nodes. The second characteristic is the increased accuracy of the method, which increases with the number of interpolation nodes. This suggests the possibility of constructing a nonlinear indicial prediction tool the accuracy of which improves with experience. "Experience" in this context is defined by the number of available indicial responses. These responses can, in principle, be inferred from experiment, CFD, or analysis, whichever is available or appropriate. As more and more indicial functions become available, the accuracy of the model increases accordingly.

Finally, and as a note of caution, it should be stressed that the actual number of indicial functions required to accurately characterize a nonlinear system, such as a maneuvering aircraft at high angles-of-attack and/or high roll rates, will depend on the nature of the system itself. For instance, the indicial function space associated with the Goman-Khrabrov system admits variations which are considerably smoother than those observed in the case of an artificial neural network trained on dynamic stall (see Refs. 13 and 14). Thus, it is expected that the indicial function space in other systems may require finer sampling, in order to generate accurate predictions. Regardless, the use of the Goman-Khrabrov system in this study has permitted the development of the basic framework for multidimensional parameterization and nonlinear interpolation of the indicial function space. The special issues concerning the handling of aerodynamic bifurcations or critical states have not been addressed in this example, and will be the object of a future paper (Ref. 14).

7. SUMMARY

A nonlinear indicial prediction model was developed to predict unsteady aerodynamic responses. The model is based on nonlinear indicial response theory and on functional interpolation of parameterized responses. Inputs to the model are the time-dependent state variables and the prerecorded nodal indicial responses of the system. The outputs of the model are the unsteady aerodynamic load time histories in response to arbitrary schedules of the state variables. The nonlinear indicial prediction method was applied to a model problem consisting of a single degree of freedom aerodynamic system (the Goman-Khrabrov model) which was fine-tuned to mimic the aerodynamic characteristics of "Cobra"-type flight test maneuvers of a fighter aircraft at high angles of

attack. The validation of the method involved recording a finite number of indicial functions which were subsequently used to construct the flow response to arbitrary schedules of $\alpha(t)$. One of the important findings of this study is that, based on the examples considered thus far, efficient parameterization of the indicial function space can be achieved based only on local information, such as the instantaneous angle of attack and pitch rate. This "local parameterization" is believed to be an essential step in the feasibility of the method, although this requires further verification using a variety of aerodynamic systems of practical interest.

For future flight simulation applications, the nonlinear indicial prediction method has the potential of being considerably faster than CFD since it involves only functional interpolation and the calculation of a generalized convolution integral. The method also becomes increasingly accurate as more indicial functions become available. With the advent of new control technologies, new and unconventional maneuvers at high rates and high angles of attack are to be expected. In these cases, conventional methods (e.g., dynamic derivatives) may not be capable of modeling accurately the key physics. The present nonlinear indicial prediction method provides a rational foundation to model off-line the nonlinear, unsteady, high angle-of-attack aerodynamics which may characterize future aircraft flight engagements, while retaining a fidelity to the flow physics of which conventional models are incapable.

ACKNOWLEDGMENT

This work was supported by Wright Laboratory under Phase I SBIR Contract F33615-95-C-3603. The author wishes to thank Capt. Deborah S. Grismer and Mr. Jerry E. Jenkins for their valuable contributions during this project.

REFERENCES

1. Nixon, D.: Alternative Methods for Modeling Unsteady Transonic Flows, *Unsteady Transonic Aerodynamics*, Vol. 120 of Progress in Astronautics and Aeronautics, Ed. by D. Nixon, AIAA, 1989.
2. Lesieutre, D. J., Reisenthel, P. H., and Dillenius, M. F. E.: Unsteady Simulation of Flexible Missiles Flying Low Over the Sea, AIAA Paper No. 94-0720, 1994.
3. Lesieutre, D. J., Reisenthel, P. H., and Dillenius, M. F. E.: A Practical Approach for Calculating Aerodynamic Indicial Functions with a Navier-Stokes Solver, AIAA Paper No. 94-0059, January 1994.
4. Reisenthel, P. H., Lesieutre, D. J., and Nixon, D.: Prediction of Aeroelastic Effects for Sea-Skimming Missiles with Flow Separation, AIAA Paper No. 91-1052, April 1991.
5. Reisenthel, P. H. and Nixon, D.: Application of Indicial Theory to the Prediction of Unsteady Separation, AIAA Paper No. 91-1742, June 1991.
6. Reisenthel, P. H.: Towards a Semi-Analytic Tool for the Prediction of Dynamic Stall, AIAA Paper No. 94-0537, 1994.
7. Tromp, J. C. and Jenkins, J. E.: A Volterra Kernel Identification Scheme Applied to Aerodynamic Reactions, AIAA Paper No. 90-2803, August 1990.
8. Silva, W. A.: A Methodology for Using Nonlinear Aerodynamics in Aeroservoelastic Analysis and Design, AIAA Paper No. 91-1110, 1991.
9. Karmakar, S.B.: Approximate Analysis of Nonlinear Systems by Laplace Transform, *J. Sound and Vib.*, Vol. 69, No. 4, pp. 597-602.
10. Tobak, M., Chapman, G. T., and Schiff, L. B.: Mathematical Modeling of the Aerodynamic Characteristics in Flight Dynamics, NASA TM 85880, 1984.
11. Tobak, M. and Chapman, G. T.: Nonlinear Problems in Flight Dynamics Involving Aerodynamic Bifurcations, NASA TM 86706, 1985.
12. Jenkins, J. E. and Myatt, J. H.: Modeling Nonlinear Aerodynamic Loads for Aircraft Stability and Control Analysis, AGARD Report 789, pp. 13/1-13/10, February 1993.
13. Reisenthel, P. H.: Novel Application of Nonlinear Indicial Theory For Simulation and Design of Maneuvering Fighter Aircraft, NEAR TR 502, November 1995.
14. Reisenthel, P. H.: Application of Nonlinear Indicial Modeling to the Prediction of a Dynamically Stalling Wing, abstract submitted for presentation at the 14th AIAA Applied Aerodynamics Conference, June 17-20, 1996, New Orleans, Louisiana.

15. Goman, M. and Khrabrov, A.: State-Space Representation of Aerodynamic Characteristics of an Aircraft at High Angles of Attack, *J. Aircraft*, Vol. 31, No. 5, 1994, pp. 1109-1115.
16. Jumper, E. J., Schreck, S. J., and Dimmick, R. L.: Lift-Curve Characteristics for an Airfoil Pitching at Constant Rate, *J. Aircraft*, Vol. 24, No. 10, 1987, pp. 680-687.
17. Ioselevich, A. S., Stolyarov, G. I., Tabachnikov, V. G., and Zhuk, A. N.: Experimental Investigation of Delta Wing $A = 1.5$ Damping in Roll and Pitch at High Angles of Attack, *Proceedings of the TsAGI*, Issue 2290, Moscow, 1985, pp. 52-70.
18. Ericsson, L. E.: Cobra Maneuver Unsteady Aerodynamic Considerations, *J. Aircraft*, Vol. 32, No. 1, 1995, pp. 214-216.
19. Shampine, L. F., Watts, H. A., and Davenport, S.: Solving Non-Stiff Ordinary Differential Equations - The State of the Art, Sandia National Laboratories Report SAND75-0182.
20. Gendrich, C. P., Koochesfahani, M. M., and Visbal, M. R.: Effects of Initial Acceleration on the Flow Field Development Around Rapidly Pitching Airfoils, *J. Fluids Engineering*, March 1995, Vol. 117, pp. 45-49.
21. Blow, K. J. and Wood, D.: Theoretical Description of Transient Stimulated Raman Scattering in Optical Fibers, *IEEE J. Quantum Electronics*, Vol. 25, No. 12, December 1989, pp. 2665-2673.
22. Algorithm 660, Collected Algorithms from ACM, Transactions on Mathematical Software, Vol. 14, No. 2, p. 149.
23. Faller, W. E. and Schreck, S. J.: Unsteady Fluid Mechanics Applications of Neural Networks, AIAA Paper No. 95-0529, January 1995.

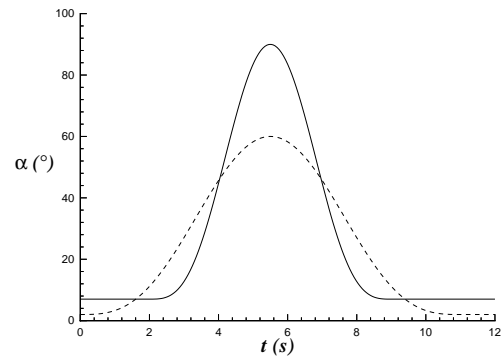


Figure 1. Analytical Approximations for Two Rapid High Angle-of-Attack Maneuvers.

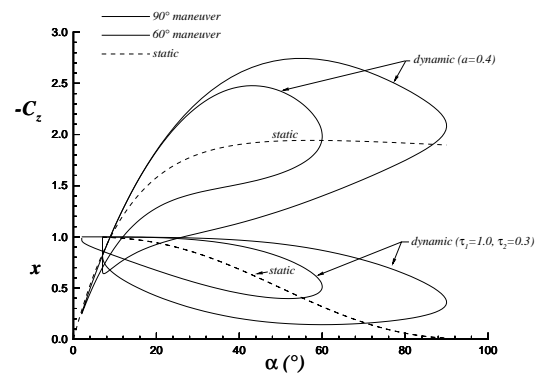


Figure 2. Prediction of Vertical Aerodynamic Force C_z and Internal State Variable x for the Two Maneuvers Shown in Figure 1.

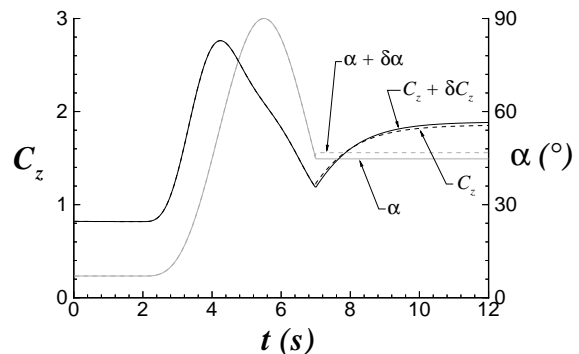


Figure 3. Illustration of the Procedure Used to Determine the Indicinal Responses.

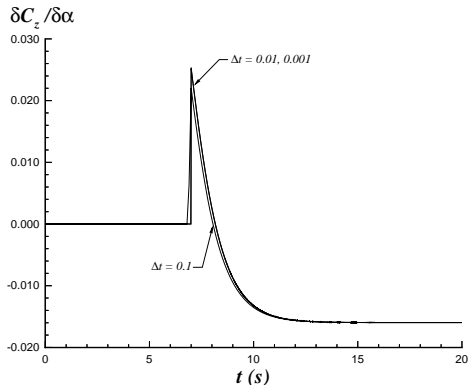


Figure 4. Convergence of the Indicial Response with Integration Time Step.

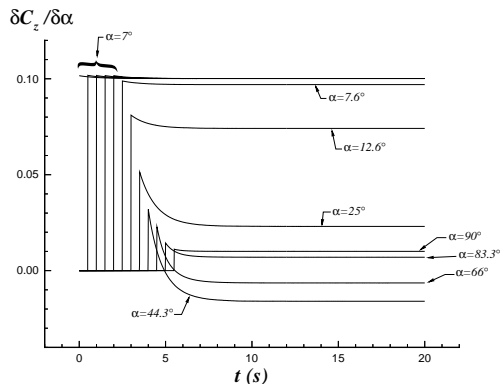


Figure 5a. Pitch Up Indicial Responses for the Large Amplitude Cobra Maneuver.

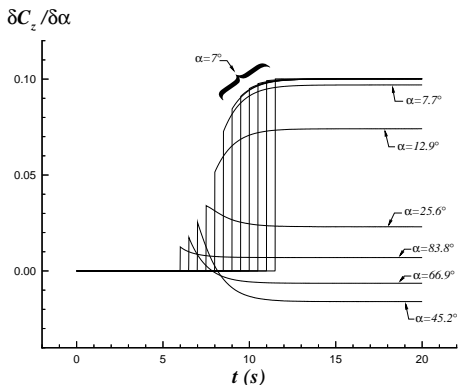


Figure 5b. Pitch Down Indicial Responses for the Large Amplitude Cobra Maneuver.

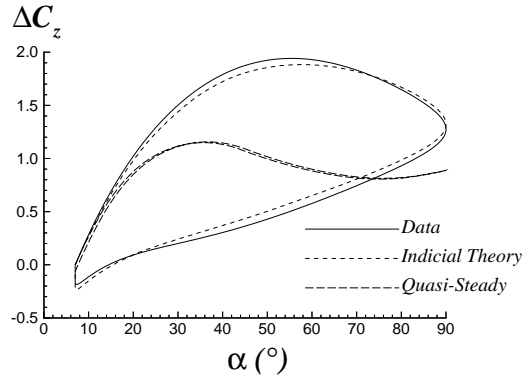


Figure 6. Hysteresis Plot of Indicial Theoretical Prediction Versus Data, Large Amplitude Cobra Maneuver.

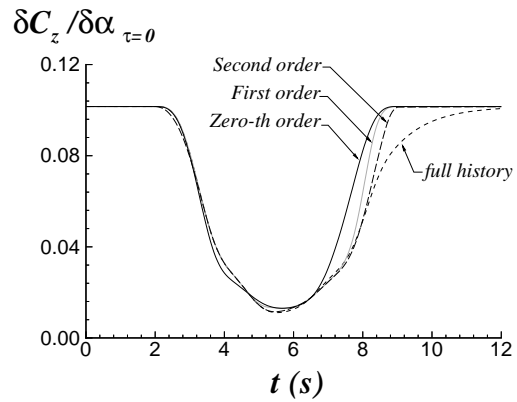


Figure 7. Effect of Indicial Ramp Order on $\delta C_z / \delta \alpha$ at $\tau=0$.

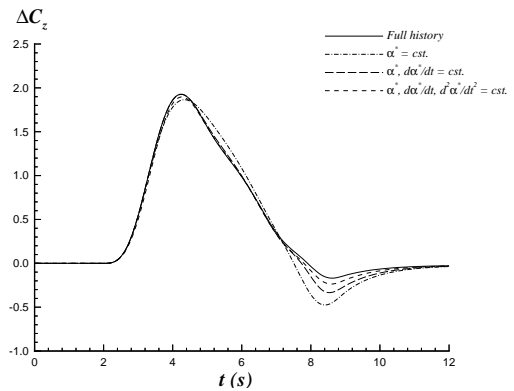


Figure 8. Effect of Indicial Ramp Order on ΔC_z Prediction, Large Amplitude Cobra Maneuver.

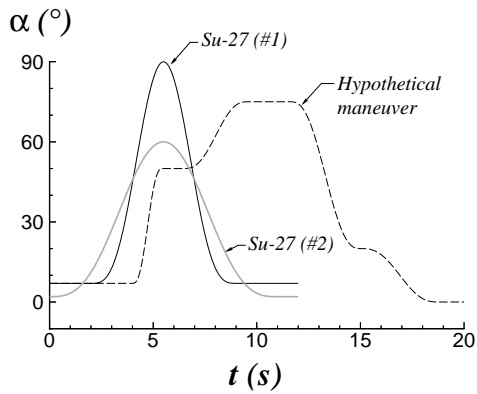


Figure 9. Time Histories of Three Pitch Plane Test Maneuvers.

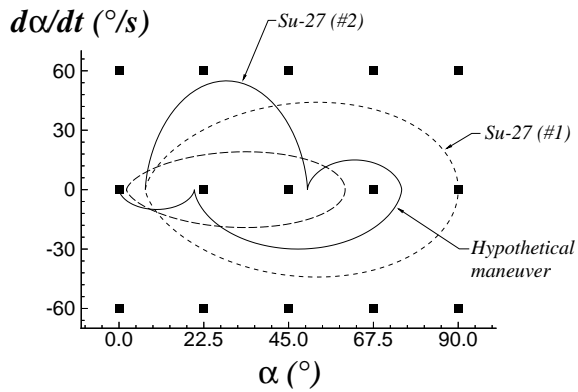


Figure 10. Illustration of Maneuver Trajectories in Parameter Space. (Filled symbols indicate the location of the interpolation nodes).

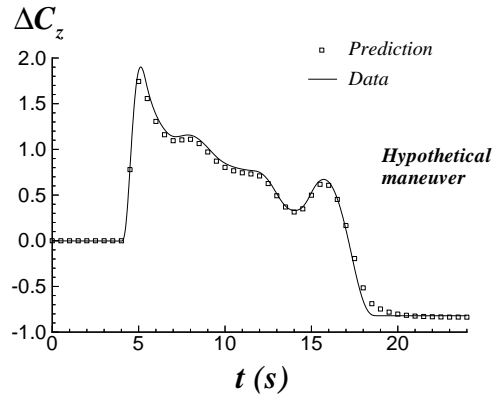


Figure 11. Accuracy of Prediction Scheme Based on $(\alpha, d\alpha/dt)$ Fifteen-Node Bi-Cubic Interpolation.

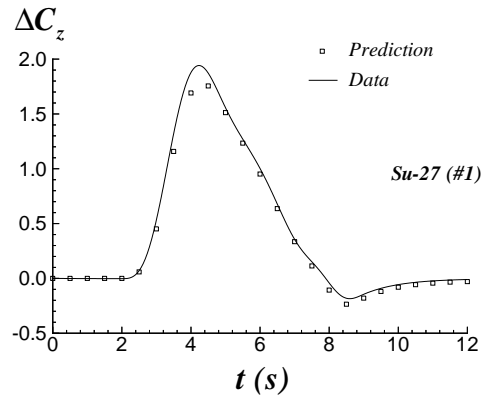


Figure 12. Accuracy of Prediction Scheme Based on $(\alpha, d\alpha/dt)$ Fifteen-Node Bi-Cubic Interpolation.

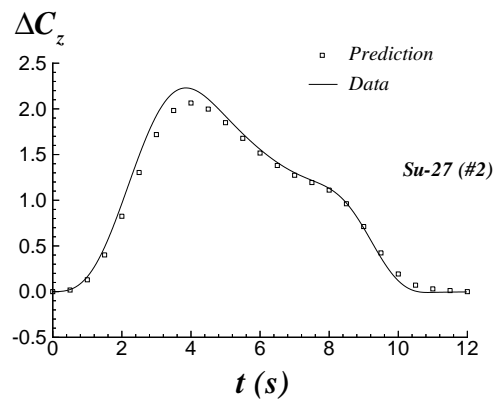


Figure 13. Accuracy of Prediction Scheme Based on $(\alpha, d\alpha/dt)$ Fifteen-Node Bi-Cubic Interpolation.

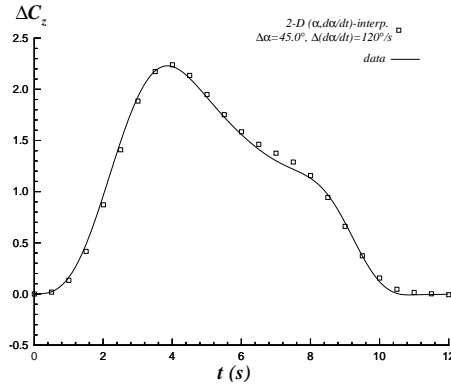
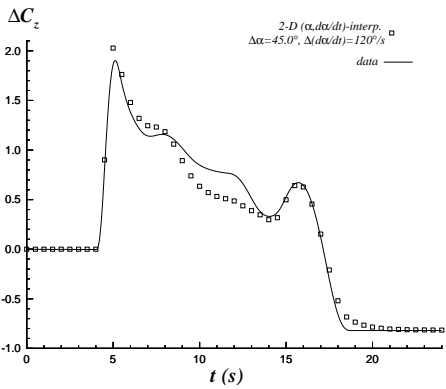
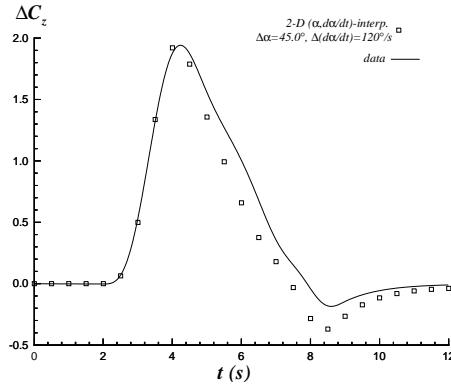
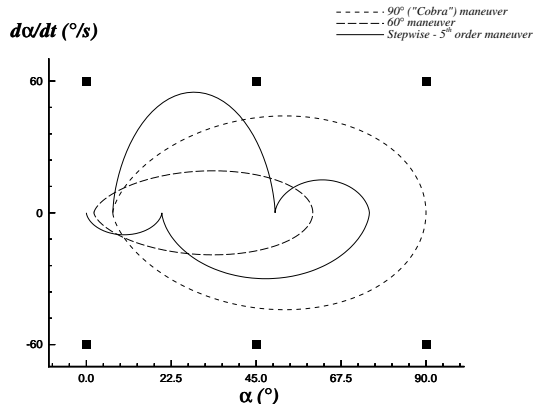


Figure 14. Accuracy of Prediction Scheme Based on $(\alpha, d\alpha/dt)$ Six-Node Bi-Cubic Interpolation. (Interpolation Nodes Are Indicated by the Filled Squares in the Upper Left Figure. Lower Left Maneuver Is "Stepwise" Maneuver; Upper Right Maneuver Is "Su27 #1"; Lower Right Is "Su27 #2").

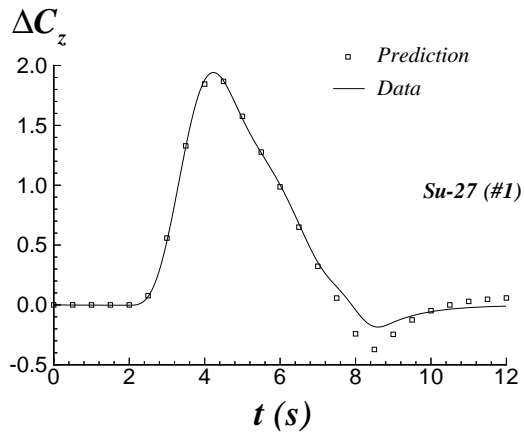
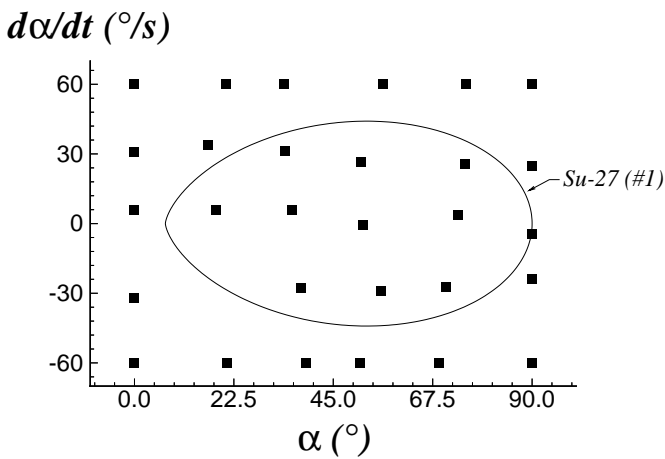


Figure 15. Accuracy of Prediction Scheme Based on $(\alpha, d\alpha/dt)$ Modified Shepard Quadratic Interpolation, Large Amplitude Cobra Maneuver. (The Prediction is Based on the Interpolation Nodes Shown in the Left Graph).